MIT-CTP 3639

Hadronic Modes and Quark Properties in the Quark-Gluon Plasma

M. Mannarelli* and R. Rapp

Cyclotron Institute and Physics Department,
Texas A&M University, College Station, Texas 77843-3366

(Dated: February 2, 2008)

Abstract

Based on interaction potentials between a heavy quark and antiquark as extracted from recent QCD lattice calculations, we set up a Brueckner-type many-body scheme to study the properties of light (anti-) quarks in a Quark-Gluon Plasma at moderate temperatures, $T \simeq$ 1-2 T_c. The quark-antiquark T-matrix, including both color-singlet and -octet channels, and corresponding quark self-energies and spectral functions are calculated self-consistently. The repulsive octet potential induces quasiparticle masses of up to 150 MeV, whereas the attractive color-singlet part generates resonance structures in the q-$\bar{q}$ T-matrix, which in turn lead to quasiparticle widths of ∼200 MeV. This corresponds to scattering rates of ∼1 fm^{-1} and may reflect liquid-like properties of the system.

PACS numbers: 25.75.-q, 25.75.Dw, 25.75.Nq

arXiv:hep-ph/0505080v2 1 Sep 2005

*Present address: Center for Theoretical Physics, Laboratory for Nuclear Science and Department of Physics Massachusetts Institute of Technology, Cambridge, MA 02139.

I. INTRODUCTION

A central goal of the relativistic heavy-ion collision program is the creation and identification of new forms of highly excited nuclear matter, in particular a deconfined and chirally symmetric Quark-Gluon Plasma (QGP). At sufficiently high temperature T, due to asymptotic freedom of Quantum Chromodynamics (QCD), the QGP is expected to be a weakly interacting gas of quark- and gluon-quasiparticles with comparatively small thermal masses, $m_{q,g} \sim gT$. Recent data from the Relativistic Heavy-Ion Collider (RHIC) indicate, however, that the produced matter exhibits strong collective behavior which is incompatible with a weakly interacting QGP: standard ($2 \leftrightarrow 2$) perturbative QCD (pQCD) cross sections for quarks and gluons do not allow for rapid thermalization [1] as required in hydrodynamic models to reproduce the observed magnitude of the elliptic flow [2, 3, 4]. With estimated initial energy densities well in excess of the critical one predicted by lattice QCD (lQCD), $\epsilon_c \simeq 1$ GeV/fm^3, the question arises what the nature of the produced medium at temperatures $T \simeq$ 1-2 T_c is ($T_c \simeq 170$ MeV: critical temperature). Of particular importance is the identification of the relevant interactions that can lead to sufficiently large scattering rates while maintaining consistency with the QGP equation of state (EoS), as determined in lQCD.

Recent (quenched) lQCD calculations found intriguing evidence that mesonic correlation functions, after transformation into Minkowski space, exhibit resonance (or bound-state) like structures for temperatures up to $\sim 2\,T_c$. This was first observed for low-lying charmonia (η_c, J/ψ) [5, 6, 7], but subsequently also for mesonic systems with lighter quarks [8, 9]. As is well known, resonance scattering is typically characterized by isotropic angular distributions and thus more efficient in randomizing momentum distributions than forward-dominated pQCD cross sections. Indeed, a recent calculation [10] based on the assumption of resonant "D"-meson states in the QGP has shown that thermal relaxation times for charm quarks are reduced by a factor of $\sim$3 as compared to using perturbative rescattering cross sections. The possibility of light hadronic states (especially for the pion and its chiral partner σ) surviving above the phase transition has been suggested some time ago using effective quark interactions, *e.g.*, within the Nambu-Jona-Lasinio model [11, 12], within the instanton-liquid model based on euclidean correlators [13], or more recently in Refs. [14, 15].

To make closer contact to lQCD, some recent works have extracted a (color-singlet) heavy-quark (Q-$\bar{Q}$) potential, V_1, from the corresponding lQCD free energy, F_1, at finite T, and injected it into a Schrödinger equation to infer quarkonium properties [16, 17, 18]. Reasonable consistency was found in that the heavy-quark bound states dissolve at roughly the same temperatures at which the peaks in the lQCD spectral functions disappear ($\sim 2\,T_c$ for J/ψ and η_c), provided the free energy was converted into a potential by subtracting an entropy term according to $V_1 = F_1 - T\, dF_1/dT$. A similar approach has also been applied to the light-quark sector in Refs. [19, 20, 21], where the q-$\bar{q}$ potentials from unquenched lQCD (including colored channels) have been supplemented by relativistic (and instanton-induced) interaction corrections. Assuming rather large quark- and gluon-quasiparticle masses, $m_{q,g} \simeq$ 3-4 T (motivated by lQCD calculations of temporal masses [22]), light mesonic, as well as a large number of colored diquark, quark-gluon and gluon-gluon, bound states have been found. Both quark-/gluon-quasiparticles and binary bound states together were shown to approximately reproduce the EoS from lQCD. However, the effects of finite widths for both (anti-) quarks and bound states, which are essential to address scattering problems, were not included.

In the present article we employ quark-antiquark potentials extracted from lQCD (including relativistic corrections as in Refs. [19, 20, 21]) within a 3-dimensionally reduced Bethe-Salpeter equation to evaluate (anti-) quark interactions in the QGP. We compute the pertinent scattering (T-) matrices in both color-singlet and -octet channels and calculate the quark self-energies including both real and imaginary parts (corresponding to quasiparticle masses and widths). The self-energies, in turn, are reinserted into the q-$\bar{q}$ propagator of the T-matrix equation, constituting a self-

consistency problem which we solve by numerical iteration. We comment on possible consequences of our results for quasiparticle masses and widths with respect to the QGP EoS and (anti-) quark rescattering timescales, respectively.

Our article is organized as follows. In Sec. II we present our parametrization of lQCD data for the singlet free energy and extract a pertinent quark-antiquark potential including both color-singlet and -octet contributions. In Sec. III we set up our self-consistency problem comprising the q-$\bar{q}$ scattering equation and in-medium single particle self-energies and propagators, and discuss the underlying assumptions and approximations. The numerical results with accompanying discussion for the T-matrix and self-energy in a nonperturbative QGP are contained in Sec. IV. In Sec. V we conclude and give an outlook.

II. QUARK-ANTIQUARK POTENTIAL FROM LATTICE QCD

To obtain a driving term (potential) for a q-$\bar{q}$ scattering equation we take recourse to lQCD calculations of the static free energy for a Q-$\bar{Q}$ pair. The Bielefeld group has performed extensive studies of this quantity based on Polyakov loop correlators [23] for both the pure-glue $SU(3)$ [24, 25] and N_f=2-QCD [26, 27]. Various parameterizations thereof have been given in the literature, cf., *e.g.*, Refs. [17, 28, 29, 30]. For the temperature range $T = 1.1$-$2\ T_c$, it turns out that unquenched

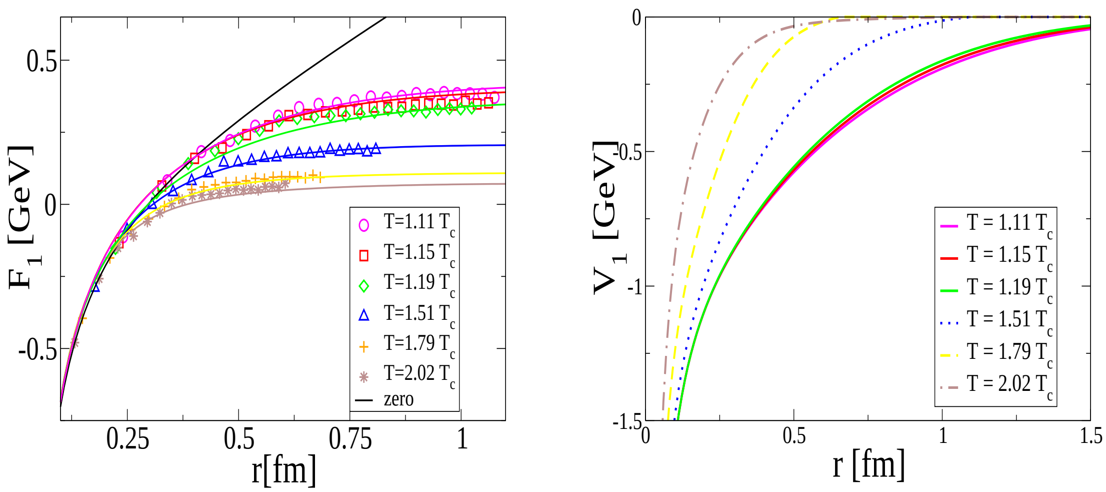

FIG. 1: Left panel: lattice QCD results for the color-singlet free energy from unquenched simulations [27] for 6 different values of the temperature (symbols) compared to our fit function, Eq. (1), represented by the various curves. Right panel: corresponding potential in the color-singlet channel obtained with Eq. (5) for the 6 different values of the temperature.

singlet free energy [26, 27] can be reasonably well reproduced by the the following form reminiscent of a screened Cornell potential (as suggested, *e.g.*, in Ref. [28]),

$$F_1(r,T) = -\frac{\alpha}{r} e^{-a\mu(r,T)r} + \frac{\sigma}{\mu(r,T)} (1 - e^{-\mu(r,T)r}) \,, \tag{1}$$

with a “screening mass”

$$\mu(r,T) = \frac{\sigma}{b} e^{-0.3/r} \tag{2}$$

and two fitting functions given by

$$a \equiv a(r,T) = \frac{1}{2\sqrt{\mu(r,T)}} \qquad\qquad b \equiv b(t) = 1.1 - 3.6\,t - 4.3\,t^2 + 17.5\,t^3 \tag{3}$$

where $t = T/T_c$, $\alpha = 0.4$ and $\sigma = 1.2\,\mathrm{GeV}^2$. The left panel of Fig. 1 summarizes our fit to the lattice "data". Also shown is the unquenched zero-temperature potential as obtained in Ref. [29] (recall that for T=0, $E_1 = F_1$, see also below), which is used to normalize the finite-T results at short distances, $r < 0.2$ fm, where the free energy is not expected to depend on temperature anymore. Our parametrization, Eq. (1), accommodates this T=0 constraint.

As mentioned in the Introduction, the appropriate quantity in relation to the free energy that can serve as an effective potential appears to be the (color-singlet) internal energy E_1. Following Kaczmarek *et. al.* [25], we subtract the entropy contribution to the free energy according to

$$E_1 \;=\; F_1 - T\frac{dF_1}{dT}\,. \tag{4}$$

The nonzero asymptotic value of the internal energy can now be interpreted as an in-medium quark mass that should not be included in the interaction part of the potential. One therefore assumes that the potential in the color-singlet channel can be extracted via

$$V_1(r,T) = E_1(r,T) - E_1(\infty,T)\,. \tag{5}$$

The singlet potential is shown in the right panel of Fig. 1 for the same values of temperature as the singlet free-energy (left panel). The potentials are appreciably larger in magnitude than the corresponding free energies and decrease with increasing temperature.

To illustrate uncertainties in the determination of the potentials we compare in Fig. 2 our results with the ones obtained by other groups for temperatures of 1.5 T_c (left panel) and 2 T_c (right panel). While the potentials of Refs. [17] (Wo) and [18] (MP) are extracted from quenched lQCD, the one of Ref. [21] (SZ) and ours (MR) result from unquenched simulations. At 1.5 T_c our potential is about 30-40% more attractive than SZ at distances between 0.1-0.8 fm, while

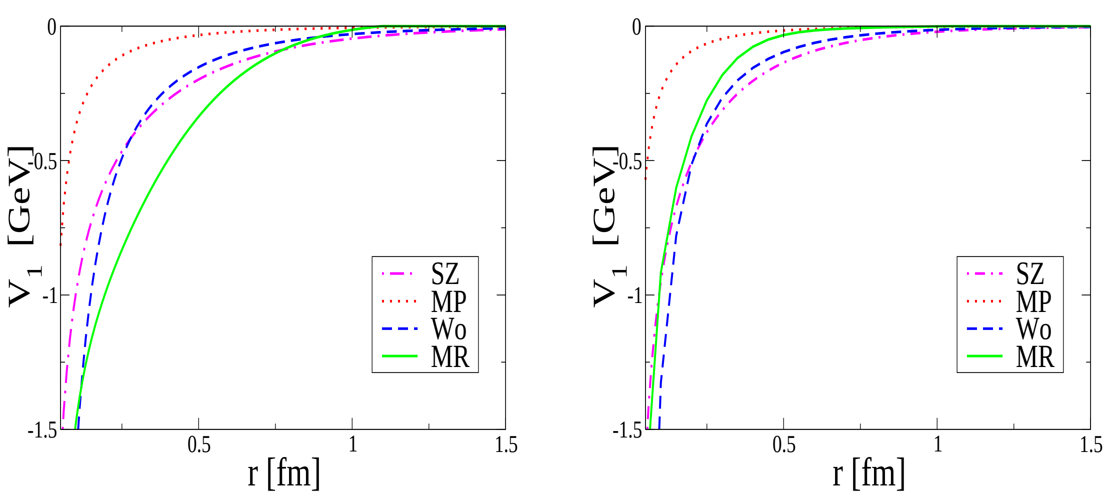

FIG. 2: Comparison of Q-$\bar{Q}$ color-singlet potentials as determined from various lattice data in our (MR) and other works (SZ [21], MP [18] and Wo [17]); the left (right) panel is for $T = 1.5\,T_c$ $(2\,T_c)$.

similar deviations also occur between the quenched-based results, while at 2 T_c our potential is less attractive than both the quenched (Wo) and unquenched (SZ) results. We therefore conclude that the current uncertainty in the extraction of the potentials amounts to about 50%, and that it does not yet allow for a systematic discrimination between quenched and unquenched results (provided the temperature dependence is normalized to T_c, which is, of course, quite different in quenched (∼260 MeV) and unquenched (∼170 MeV) simulations). The pertinent uncertainties will be assessed below by performing T-matrix calculations for charmonium (c-$\bar{c}$ systems) with both our and the quenched Wo potential (cf. Sect. IV A), and comparing them to spectral functions from lQCD [6] obtained with different methods; reasonable agreement will be found.

Toward a more complete description of the q-$\bar{q}$ interactions in the QGP we will in this work also consider the (repulsive) contributions from the color-octet channel. However, as pointed out in Ref. [31], the octet potential cannot be straightforwardly inferred from the Polyakov loop correlators. Due to a lack of better knowledge of the octet free energies, we here assume that the octet potential follows the leading-order result of perturbation theory,

$$F_8 = -\frac{1}{8} F_1 \,. \tag{6}$$

Again, we will check the sensitivity of our calculations to this approximation, by varying the coefficient in Eq. (6) by a factor of 0.5-2.

For non-static quarks it is also important to include relativistic corrections [20, 32]. Following Ref. [20] we implement a velocity-velocity interaction term by the replacement $V(r) \to V(r)(1 - \hat{\alpha}_1 \cdot \hat{\alpha}_2)$ where $\hat{\alpha}_1$ and $\hat{\alpha}_2$ are quasiparticle velocity operators. As pointed out in Ref. [21], this procedure is strictly speaking correct only for a Coulomb-type potential.

III. REDUCED BETHE-SALPETER EQUATION, QUARK SELF-ENERGY AND SELF-CONSISTENCY

To evaluate quark-antiquark interactions in the QGP we employ the T-matrix approach, as is well known from the nuclear many-body problem. In relativistic field theory, the starting point is a 4-dimensional Bethe-Salpeter (BS) equation,

$$T = K + \int KSST \,, \tag{7}$$

where K denotes the interaction kernel and S is the single-particle propagator. Both quantities carry, in principle, dependencies on temperature and (baryon-) density of the surrounding medium. Since the effective q-$\bar{q}$ potential constructed in the previous section is essentially non-relativistic in nature, it is appropriate to employ the ladder approximation to Eq. (7) in connection with neglecting virtual particle-antiparticle loops. Thus, we will identify the kernel K with the potential V with appropriate approximations in the propagator and scattering equation to be discussed in the following.

The medium effects in the quark propagator, S, are encoded in a self-energy which we decompose according to

$$\Sigma = \tilde{\Sigma} + \int TS \,. \tag{8}$$

The first term, $\tilde{\Sigma}$, represents a "gluon-induced" contribution due to interactions of (anti-) quarks with surrounding thermal gluons. In this work we do not calculate this term explicitly, but we will study how different (purely real) values affect our results. We note that a perturbative (hard-thermal-loop) form of this (mass-) term is widely used as a parameter in quasiparticle descriptions

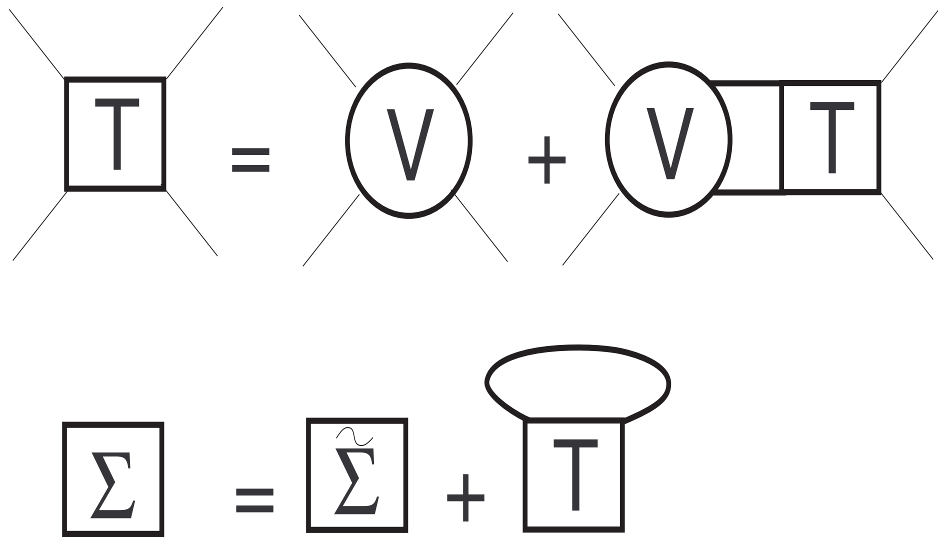

FIG. 3: Schematic representation of the self-consistency problem composed of the Bethe-Salpeter equation (7) in ladder approximation and the quark self-energy, Eq. (8). Thick lines represent full fermionic propagators. The four different blocks correspond to the T-matrix (T), potential (V), self-energy (Σ) and "gluon-induced" self-energy ($\tilde{\Sigma}$).

of the QGP EoS [33, 34, 35, 36]. The second term on the right side of Eq. (8) is the contribution to the self-energy induced by interactions with antiquarks of the heat bath which we compute at the same level of approximation as the T-matrix. In principle, the quark self-energy also receives contributions from interactions with thermal quarks (which could be significant especially in the scalar diquark channel), but we neglect them in this work. We also constrain ourselves to the case of vanishing quark chemical potential, $\mu_q = 0$, which implies equal self-energies for quarks and antiquarks. The two equations (7) and (8) constitute a self-consistency problem which is diagrammatically illustrated in Fig. 3.

Let us discuss the single-particle quantities in more detail. The full quark propagator obeys a Schwinger-Dyson equation,

$$S = S_0 + S_0 \Sigma S \,, \tag{9}$$

where $S_0(k) = [\not{k} - m_0]^{-1}$. In the following, we set the current quark mass, m_0, to zero and assume the self-energy to take the (chirally invariant) form

$$\Sigma(\omega, \mathbf{k}) = a(\omega, k)\gamma_0 + b(\omega, k)\hat{\mathbf{k}} \cdot \gamma \,, \tag{10}$$

since scalar and tensor contributions are suppressed due to chiral symmetry restoration (above T_c), whereas pseudoscalar and axialvector terms are absent due to parity invariance. The self-energy can be further decomposed as (cf., *e.g.*, Ref. [37])

$$\gamma_0 \Sigma(\omega, \mathbf{k}) = \Sigma_+(\omega, k)\Lambda_+(\hat{\mathbf{k}}) - \Sigma_-(\omega, k)\Lambda_-(\hat{\mathbf{k}}) \;, \tag{11}$$

where

$$\Lambda_\pm(\hat{\mathbf{k}}) = \frac{1 \pm \gamma_0 \hat{\mathbf{k}} \cdot \gamma}{2} \tag{12}$$

are projectors on quark states with chirality equal (Λ_+) or opposite (Λ_-) to their helicity, and $\Sigma_\pm = b(\omega,k) \pm a(\omega,k)$. The quark propagator then follows as

$$S(\omega,k)\gamma_0 = \Delta_+(\omega,k)\Lambda_+(\hat{\mathbf{k}}) + \Delta_-(\omega,k)\Lambda_-(\hat{\mathbf{k}}) \tag{13}$$

with $\Delta_\pm = -(\omega \mp (k+\Sigma_\pm))$. Since the potential extracted from lQCD is independent of chirality, the self-energy satisfies $\Sigma_+ = -\Sigma_-$, that is $b(\omega,k) = 0$. Recalling Eq. (10), this implies that the non-perturbative interactions only contribute to a chirally invariant (thermal) mass term for anti-/quarks. For the "gluon-induced" self-energy, $\tilde{\Sigma}$ in Eq. (8), we adopt a form suggested by the high-temperature hard-thermal loop result, characterized by a mass term, m, in the pertinent dispersion relation,

$$\omega_k = \sqrt{k^2+m^2}\ , \tag{14}$$

ignoring possible imaginary parts. Our default value for m is 0.1 GeV.

Let us now turn to the scattering equation (7). As mentioned above, we neglect the (virtual) antiparticle components in the quark propagator and apply a 3-dimensional (3-D) reduction scheme to the 4-dimensional BS equation, facilitating its numerical evaluation substantially. The resulting Lippmann-Schwinger equation takes the form

$$T_a(E;\mathbf{q}',\mathbf{q}) = V_a(\mathbf{q}',\mathbf{q}) - \int \frac{d^3k}{(2\pi)^3}\ V_a(\mathbf{q}',\mathbf{k})\ G_{q\bar{q}}(E;k)\ T_a(E;\mathbf{k},\mathbf{q})\ [1-2f(\omega_k)]\,, \tag{15}$$

where E denotes the center-of-mass (CM) energy and $\mathbf{q}$ and $\mathbf{q}'$ are the in- and outgoing (off-shell) 3-momenta in the CM (as usual, the on-shell T-matrix is defined by $q{=}q'$ with $E = 2\omega_q$ where ω_q is the on-shell single-quark energy); $a = 1,8$ labels color-singlet and -octet channels, and

$$f(\omega)\ =\ \frac{1}{e^{\omega/T}+1} \tag{16}$$

is the Fermi-Dirac distribution. The explicit form of the two-particle propagator, $G_{q\bar{q}}(E;k)$, depends on the 3-D reduction scheme. Unless otherwise stated, we adopt the Blankenbecler-Sugar (BbS) [38] prescription leading to

$$G_{q\bar{q}}(E;k) = \frac{\omega_k}{\omega_k^2 - E^2/4 + 2i\omega_k\Sigma_I(\omega_k,k)} \quad \text{(BbS)}\ , \tag{17}$$

but we have checked that our results are very similar when employing the Thompson scheme [39] with

$$G_{q\bar{q}}(E;k) = \frac{1}{2}\frac{1}{\omega_k - E/2 + i\Sigma_I(\omega_k,k)} \quad \text{(Th)}\ . \tag{18}$$

In both Eqs. (17) and (18) ω_k denotes the on-shell quasiparticle dispersion law, *i.e.*, the solution of the equation

$$\omega_k = \sqrt{k^2+m^2} + \Sigma_R(\omega_k,k)\,, \tag{19}$$

with Σ_R and Σ_I the real and imaginary part of the self-energy. Finally, the potential figuring into Eq. (15) follows from our lQCD parametrization via Fourier transformation,

$$V_a(\mathbf{q}',\mathbf{q}) = \int d^3r V_a(r) e^{i(\mathbf{q}-\mathbf{q}')\cdot\mathbf{r}}\,. \tag{20}$$

To solve Eq. (15) it is convenient to work in a partial-wave basis. Expanding T-matrix and potential,

$$V_a(\mathbf{q}',\mathbf{q}) \;=\; 4\pi\sum_l (2l+1)\; V_{a,l}(q',q)\; P_l(\mathbf{q}'\cdot\mathbf{q})\;, \tag{21}$$

$$T_a(E;\mathbf{q}',\mathbf{q}) \;=\; 4\pi\sum_l (2l+1)\; T_{a,l}(E;q',q)\; P_l(\mathbf{q}'\cdot\mathbf{q})\;, \tag{22}$$

allows to perform the angular integrations to yield

$$T_{a,l}(E;q',q) = V_{a,l}(q',q) - \frac{2}{\pi}\int k^2dk\; V_{a,l}(q',k)\; G_{q\bar{q}}(E;k)\; T_{a,l}(E;k,q)\; [1-2f(\omega_k)]\;. \tag{23}$$

In the present study we will constrain ourselves to S-wave channels, deferring higher waves to future work. In Ref. [21] it was found that P-wave bound state formation is strongly suppressed (in accordance with our own estimates). Concerning spin-isospin channels, we recall that in the chirally restored phase the spectral functions of chiral partners (*e.g.*, π-σ, ρ-a_1) degenerate, which is also reflected in the spectral functions extracted from lQCD [40]. Within the naive constituent quark model, π and ρ states are S-wave q-$\bar{q}$ bound states, whereas σ and a_1 are in a P-wave state. Interestingly, lQCD spectral functions find an additional (approximate) degeneration of π and ρ states above T_c [8, 40]. In as far as an interpretation of these objects as $q\bar{q}$ states applies, this might be taken as an indication for a spin-symmetry much like in heavy-quark effective theories. In view of these considerations, and due to the fact that our lQCD-extracted potential is flavor-blind, we will assume the color-singlet S-wave states to appear with a spin-isospin degeneracy corresponding to π+ρ states, $d_{SI}=12$. Since the color-octet potential does not carry any flavor-dependence either, the same factor will be applied to the color-octet states.

With the q-$\bar{q}$ T-matrix at hand, we can proceed to calculate the explicit expression for the quark self-energy due to interactions with anti-quarks. Within the imaginary time formalism the latter follows from closing the forward scattering T-matrix with a thermal $\bar{q}$ propagator,

$$\Sigma(z_v;p) = \frac{d_{SI}}{12}\, d_a \int \frac{d^3p'}{(2\pi)^3}\; (-T)\; \sum_{z_{\nu'}} T^a_{q\bar{q}}(z_\nu+z_{\nu'};\mathbf{p},\mathbf{p}')\; D_{\bar{q}}(z_{\nu'},\mathbf{p}') \tag{24}$$

(here, $z_\nu = \pi i(2\nu+1)T$ are fermionic Matsubara frequencies, $d_{1,8}=1,8$ is the color degeneracy factor and the factor 1/12 represents the average over the $3\times2\times2$ (color$\times$flavor$\times$spin) initial quark states). Using the spectral representations of both T-matrix and $\bar{q}$ propagator to perform the Matsubara sum, and after analytic continuation to the real axis, the self-energy takes the form

$$\Sigma_a(\omega;p) = \frac{d_{SI}}{12}\, d_a \int\frac{d\omega'}{2\pi}\int\frac{dE}{\pi}\int\frac{d^3k}{(2\pi)^3}\; A(\omega',k)\; \frac{f(\omega')+g(E)}{\omega+\omega'-E+i\eta}\; \mathrm{Im}T_a(E;\mathbf{k}+\mathbf{p}) \tag{25}$$

with the Bose distribution

$$g(E) = \frac{1}{e^{E/T}-1} \tag{26}$$

and the quark spectral function

$$A(\omega,k) = \frac{-2\,\Sigma_I(\omega,k)}{(\omega-\sqrt{k^2+m^2}-\Sigma_R(\omega,k))^2+\Sigma_I(\omega,k)^2}\,. \tag{27}$$

To further simplify our task we assume in the following a quasiparticle approximation for the spectral function,

$$A(\omega,k) \;=\; 2\pi\delta(\omega-\omega_k)\,, \tag{28}$$

where ω_k is obtained from the self-consistent solution of Eq. (19) (we will check this approximation below). If we furthermore neglect the (weak) energy dependence of $g(E)$ close to the pole of the principal value integral in Eq. (25), we can recover the real part of $T_{q\bar{q}}$ to cast the self-energy in compact form,

$$\Sigma_a(\omega;p) = \frac{d_{SI}}{12}\, d_a \int \frac{k^2 dk\, dx}{(2\pi)^2} \;\; [f(\omega_k) + g(\omega+\omega_k)]\; T^a_{q\bar{q}}(E)\,, \tag{29}$$

where $x = \cos\theta$ (with $\theta = \angle(\mathbf{p},\mathbf{k})$) and the CM energy of the on-shell T-matrix is given by

$$E = \sqrt{(\omega_k+\omega)^2 - (\mathbf{p}+\mathbf{k})^2}\,. \tag{30}$$

IV. T-MATRIX, SELF-ENERGY AND SPECTRAL FUNCTION

In this section we discuss the numerical solutions to the set of equations (19), (23) and (29). Self-consistency is achieved by iteration, starting with the calculation of the T-matrix using a constant self-energy in the first step. The self-energy is then calculated from (29) and used to solve the on-shell condition (19). The pertinent quasiparticle dispersion-law is then re-inserted into the T-matrix equation and the procedure is iterated until T-matrix and self-energy converge (typically within less than 10 iteration steps; we have also verified that the final results are insensitive to the initial input value for the self-energy).

A. Quark-Antiquark T-matrix

The T-matrix equation (23) is solved using the matrix inversion algorithm of Haftel and Tabakin [41] (after discretizing the momentum integration). To assess the possible formation of bound states, the T-matrix needs to be calculated below the nominal q-$\bar{q}$ threshold, $E_{thr} = 2(m + \Sigma_R(E_{thr}/2, 0))$. The potential does not depend on the CM energy E, and, due to its nonrelativistic character, is only defined for real external 3-momenta q and q'. We therefore define the subthreshold on-shell T-matrix by setting the external momenta q=q'=0. In the following we will refer to a peak in the imaginary part of the T-matrix as a bound-state (resonance) if the energy of the maximum is located below (above) the quasiparticle threshold, E_{thr}.

1. *Charmonium Systems*

To check the reliability of the parametrization of the potential in the singlet channel, and of the algorithm to compute the T-matrix, we first apply our approach to the c-$\bar{c}$ (charmonium) sector by using a (constant) quark mass of $m = 1.8$ GeV which approximately reproduces the vacuum J/ψ mass at the lowest temperature (note that self-consistency does not play a role here since the thermal abundance of c-quarks is strongly suppressed; for numerical purposes, we used a fixed imaginary value for the self-energy, $\Sigma_I = -10$ MeV, and $\Sigma_R = 0$). The results are displayed in Fig. 4 for three different temperatures, $1.2\,T_c$ (left panel), $1.5\,T_c$ (middle panel) and $2\,T_c$ (right panel). As the temperature increases the charmonium state moves up in energy (reflecting a decreasing binding energy) reaching the threshold ($E_{thr} = 3.6$ GeV) at $T \simeq 2\,T_c$ after which the resonance peak essentially dissolves (also note that the strength in the T-matrix is much reduced at 2 T_c as compared to the lower temperatures). This behavior is in reasonable (qualitative) agreement with both lQCD calculations [6] and effective potential models using a Schrödinger equation [17, 18].

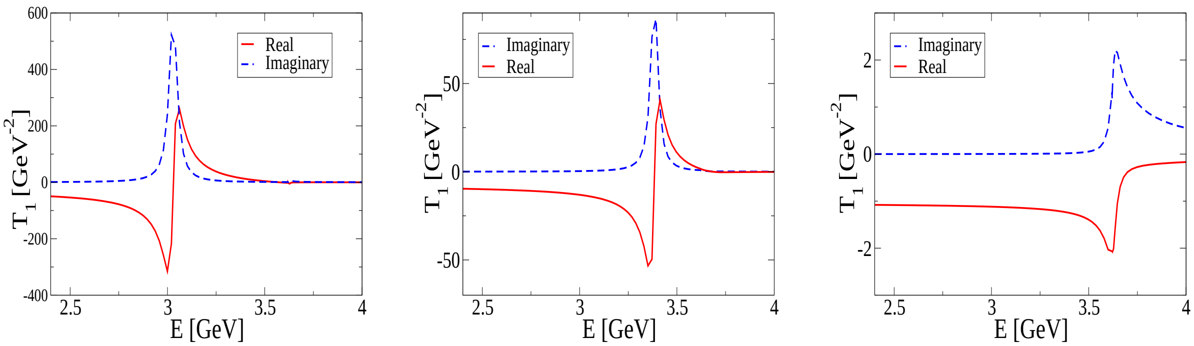

FIG. 4: Real (full red line) and imaginary part (absolute value, dashed blue line) of T-matrix in the color-singlet channel for charmonium (with a charm-quark mass of $m = 1.8$ GeV) at $T = 1.2\,T_c$, $T = 1.5\,T_c$, $T = 2\,T_c$ (left, middle and right panel, respectively) as a function of CM energy E, based on our potential parametrization extracted from unquenched lQCD.

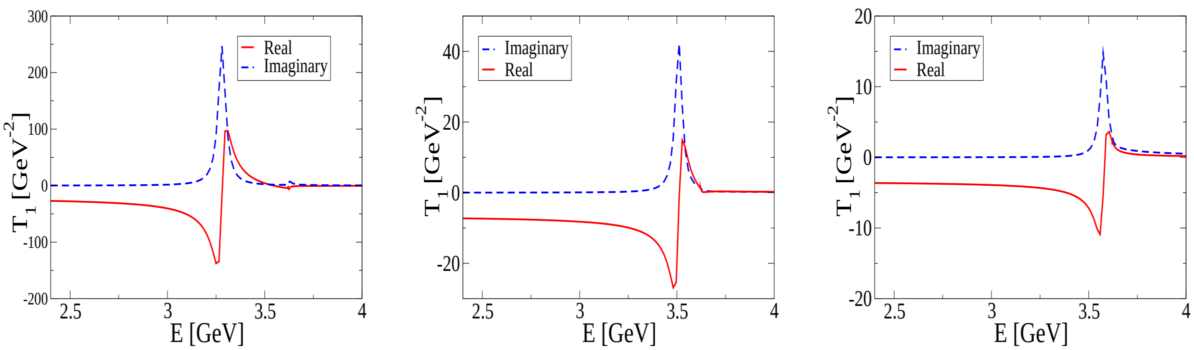

FIG. 5: Real (full red line) and imaginary part (absolute value, dashed blue line) of T-matrix in the color-singlet channel for charmonium (with a charm-quark mass of $m = 1.8$ GeV) at $T = 1.2\,T_c$, $T = 1.5\,T_c$, $T = 2\,T_c$ (left, middle and right panel, respectively) as a function of CM energy E, based on a potential [17] extracted from quenched lQCD.

To check the sensitivity to the underlying potential (recall the discussion in Sec. II around Fig. 2), we have repeated the calculations for the charmonium T-matrix in the singlet channel using the (quenched-based) potential of Ref. [17], cf. Fig. 5. At the lower temperature of $1.2\,T_c$ the binding is significantly less pronounced (by about 0.25 GeV) as compared to our parametrization, as to be expected from the less attractive potential. At higher temperatures the agreement improves, and both potentials lead to a very similar temperature where the state crosses the c-$\bar{c}$ threshold (close to $2\,T_c$), with strongly reduced strength. This, in turn, is again in line with the Schrödinger-equation approach, in which the c-$\bar{c}$ system becomes unbound around $\sim 2\,T_c$ [17]. While the resonance at $2\,T_c$ appears to be rather narrow, we recall that we did not include here (temperature dependent) absorptive parts [10] and reduced masses for the c-quarks (nor inelastic charmonium reaction channels [42]), all of which are expected to increase the width of the charmonium states.

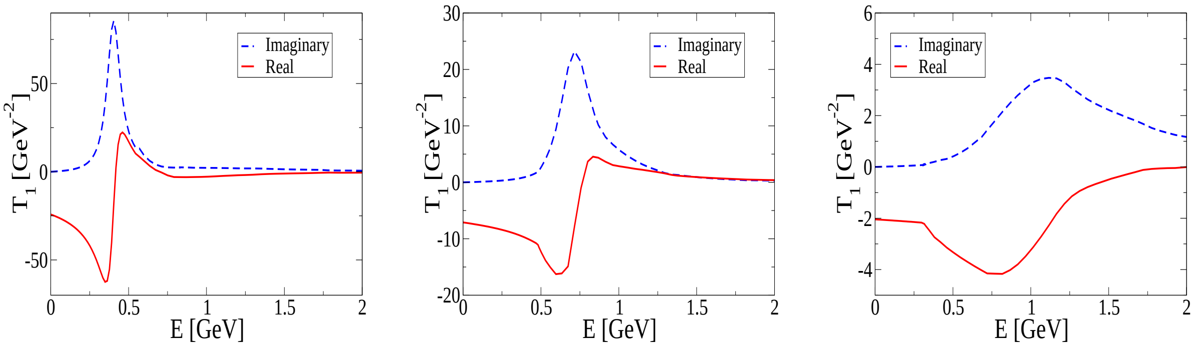

FIG. 6: Real (full red line) and (absolute value of the) imaginary part (dashed blue line) of the light-quark (on-shell) T-matrix in the color-singlet channel at temperatures $T = 1.2\,T_c$, $T = 1.5\,T_c$ and $T = 1.75\,T_c$ (left, middle and right panel, respectively) as a function of the $q\bar{q}$ CM energy E, with a "gluon-induced" quark-mass term $m = 0.1$ GeV.

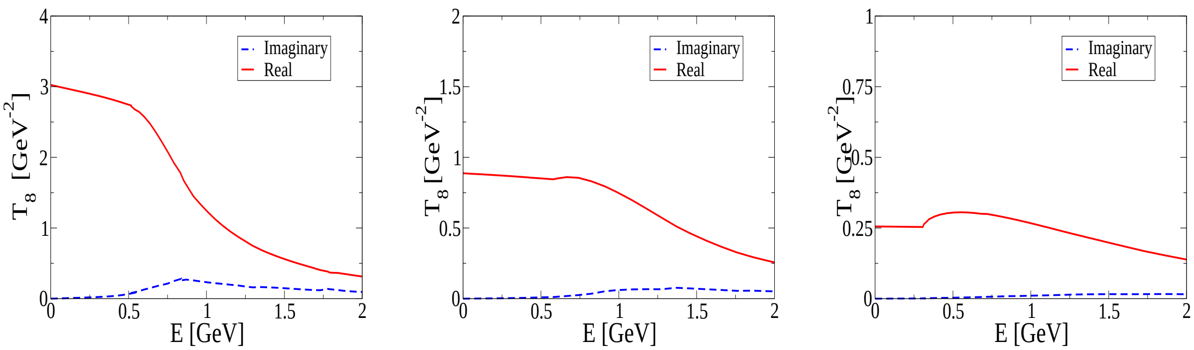

FIG. 7: Light-quark T-matrix in the color-octet channel vs. $q\bar{q}$ CM energy at $T = 1.2\,T_c$, $T = 1.5\,T_c$ and $T = 1.75\,T_c$ (left, middle and right panel, respectively) with $m = 0.1$ GeV. Solid (red) line: real part; dashed (blue) line: imaginary part (absolute value).

2. *Light-Quark Systems*

Turning to the light-quark sector, the self-consistent results for real and imaginary part of the on-shell T-matrix for quasiparticles with a gluon-induced mass-term of $m = 0.1$ GeV are summarized in Figs. 6 and 7 for temperatures $T = 1.2\,T_c$, $T = 1.5\,T_c$ and $T = 1.75\,T_c$.

At $T = 1.2\,T_c$ the color-singlet T-matrix exhibits a relatively narrow bound state located significantly below the q-$\bar{q}$ threshold energy of $E_{thr} \simeq 0.52$ GeV (corresponding to twice the real part of the total quark self-energy discussed below). When increasing the temperature to $1.5\,T_c$, the state moves to higher CM energy above the threshold ($E_{thr} \simeq 0.48$ GeV) which, not surprisingly, is accompanied by a significant broadening. Note also that the peak value is substantially reduced as compared to the $1.2\;T_c$ case, substantially more than to be expected from the broadening alone. We assign this behavior to the decrease in the potential, cf. right panel of Fig. 1, reflecting an overall reduction in interaction strength. The trends in suppression, broadening and upward energy-shift continue at $T = 1.75\,T_c$ where the resonance has now essentially melted as indicated by a width of almost 1 GeV, comparable to its mass. These results may be put into context with computations of mesonic spectral functions in (quenched) lattice QCD. For (reasonably) light quarks [8, 40], their

main features above T_c are a gradual increase of the peak position (corresponding to the "meson mass") with temperature (roughly proportional to T), accompanied by a broadening. The bound / resonance states depicted in Fig. 6 approximately share both of these features.

The T-matrix in the color-octet channel is displayed in Fig. 7 for the same set of temperatures. As to be expected for a purely repulsive potential, we find a smooth (non-resonant) dependence of both real and imaginary part with CM energy (with a substantial suppression at higher T, as in the singlet case). The imaginary part is very small, and also the real part appears to be small when compared to the singlet channel. We recall, however, that the octet contribution to the self-energy, Eq. (29), enters with a weight which is by a factor of 8 larger than for the singlet one, rendering it an important effect as will be seen below.

B. Self-Energy

We proceed to the single-quark self-energies as calculated from the interactions with antiquarks of the heat bath using the expression, Eq. (29), based on the self-consistent S-wave q-$\bar{q}$ T-matrices in the "π" and "ρ" channels as obtained in the previous section. We recall that the real part of the self-energy corresponds to a chirally invariant mass-term, whereas its imaginary part determines the width of a quark (-quasiparticle) according to $\Gamma = -2\ \mathrm{Im}\Sigma$. Since we work at zero quark-chemical potential, $\mu_q = 0$, the same results hold for antiquarks. We also recall that our on-shell approximation scheme for the self-energy implies that the effects of bound states are not captured by Eq. (29), since in the integration over the T-matrix only energies above the q-$\bar{q}$ threshold, E_{thr}, contribute.

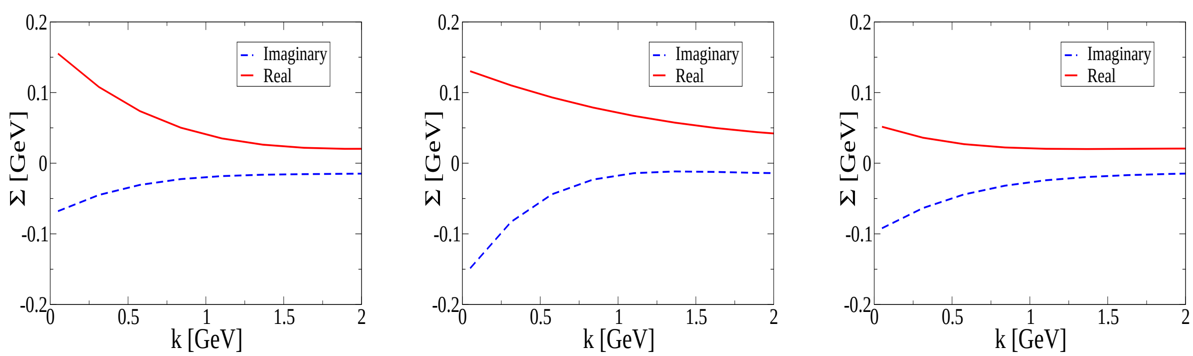

FIG. 8: Real (solid line, red) and imaginary (dashed line, blue) part of the on-shell quark self-energy as a function of 3-momentum at temperatures $T = 1.2\,T_c$, $T = 1.5\,T_c$ and $T = 1.75\,T_c$ (left, middle and right panel, respectively) with $m = 0.1$ GeV.

In Fig. 8 the on-shell self-energy is displayed for the same selection of temperatures as in the previous section. Both real and imaginary part are smooth functions of the quark 3-momentum with maximal values at $k = 0$. Note that real part is positive, implying that the repulsive contribution from the octet channels overcomes the attractive singlet channels. The imaginary part (width), on the other hand, chiefly arises due to resonant scattering in the singlet channel.

More quantitatively, in the temperature regime 1.2-1.5 T_c, the nonperturbative contribution to the thermal quark mass reaches values of around 150 MeV at small momenta, decreasing to ∼50 MeV at 1.75 T_c. With the underlying "gluon-induced" mass term of $m = 100$ MeV, the total thermal mass, $m + \Sigma_R$, amounts to 150-250 MeV. This is smaller than effective (perturbative) thermal quark masses required in phenomenological fits to the QGP EoS of lQCD [33, 34, 35, 36].

To improve upon this, we have performed self-consistent calculations with a gluon-induced mass term of $m = 250$ MeV. It turns out that, at given temperature, the "mesonic" states are slightly stronger bound, but in general the behavior of T-matrix and pertinent self-energy are quite similar to those obtained with $m = 100$ MeV. *E.g.*, for $T = 1.5\ T_c$ (cf. Fig. 9), the resonance structure is right at threshold, the quark width reaches almost 200 MeV, and the combined real part at low momenta amounts to a quark mass of $m + \Sigma_R \simeq 350$ MeV.

An important aspect of our results are the rather large imaginary parts of the quark self-energy, translating into widths of about 200 MeV at low momenta for temperatures around 1.5 T_c. As mentioned above, the width is almost entirely generated by the resonant scattering in the singlet channel; this is nicely illustrated by the significant increase in ImΣ when going from 1.2 to 1.5 T_c (cf. left and middle panel in Fig. 8), during which the state in the T-matrix moves from below to above threshold (cf. left and middle panel in Fig. 6), *i.e.*, converts from bound state to resonance[1]. The magnitude of the quark widths is quite comparable to the thermal masses, qualitatively supporting the notion that the QGP could be in a liquid-like regime [43, 44]. Even at the highest considered temperature of 1.75 T_c, and at typical thermal momenta ($k \simeq 3T \simeq 0.9$ GeV), the quark width due to scattering off antiquarks is between 50 and 100 MeV. This does neither include P-wave interactions, nor strange antiquarks, nor any contributions from scattering off quarks or gluons.

Finally let us come back to the uncertainty associated with the interaction in the octet channel related to the perturbative ansatz, Eq. (6). If the coeffiecient in Eq. (6) is increased (decreased) by a factor 2 (for $T = 1.5\,T_c$ and $m = 0.25$ GeV), the imaginary part of the self-energy barely changes, whereas its real part increases (decreases) by about a 40%.

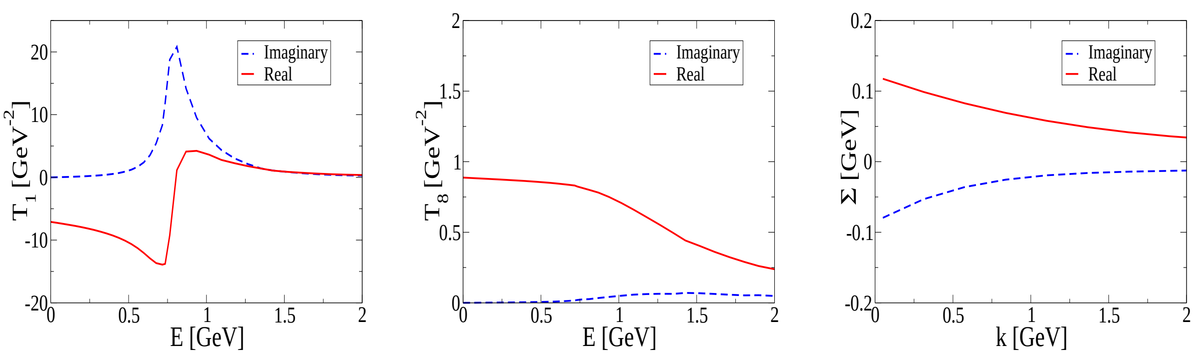

FIG. 9: Real (full line, red) and imaginary (dashed line, blue) parts of the T-matrix in the color-singlet channel (left panel), color-octet channel (central panel) and corresponding (singlet+octet) self-energy (right panel) at a temperature $T = 1.5\,T_c$ using a "gluon-induced" mass term of $m = 0.25$ GeV.

C. Quark Spectral Functions and Normalization Condition

To better elucidate the validity of the quasiparticle approximation, Eq. (28), we compute the off-shell real and imaginary parts of the self-energy using Eq. (29) and obtain the pertinent quark spectral function $A(\omega, k)$ from Eq. (27). In Fig. 10 we depict $A(\omega, k)$ as a function of quark energy,

[1] We recall that bound states are not accessible in on-shell $2 \to 2$ scattering; even if a resonance is close to threshold it does not contribute effectively to rescattering processes if the average thermal energy of particles from the heat bath is significant. The contribution of bound states to the self-energy can be included rather by going beyond the quasiparticle approximation, *i.e.*, evaluating Eq. (25) with the off-shell spectral function, Eq. (27).

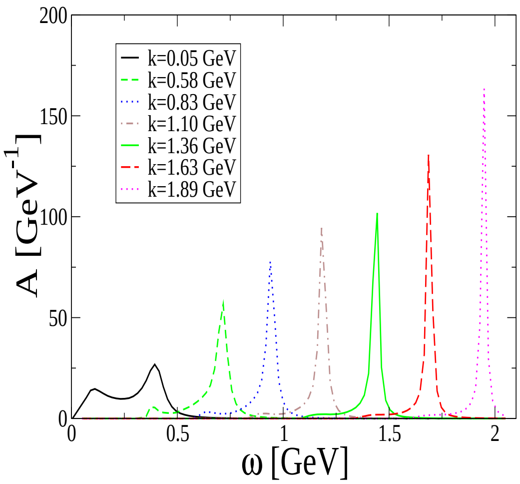

FIG. 10: Off-shell spectral function $A(\omega, k)$ as given by Eq. (27) vs. quark energy for different values of the quark momentum at $T = 1.5\,T_c$ and for $m = 0.25$ GeV.

ω, for various fixed momenta at a temperature of $T = 1.5\ T_c$. On the one hand, this reiterates the large effect of the width for low momenta and calls for an off-shell treatment to improve the reliability of our results in the (sub-) threshold region of the T-matrix. On the other hand, for larger momenta (including typical thermal momenta) the quasiparticle approximation as applied in our calculations appears to be reasonably well justified.

As another check of our approximations we have evaluated the norm of the quark spectral functions defined by

$$I(k) \ = \int \frac{d\omega}{2\pi} A(\omega, k)\,. \tag{31}$$

The unitarity condition for $A(\omega, k)$ requires $I(k) = 1$ for each momentum k. This relation is rather well satisfied, $I(k) \geq 94$ %, for all momenta considered in Fig. 10.

V. CONCLUSIONS AND OUTLOOK

In the present article we have set up a self-consistent many-body scheme of Brueckner-type to assess nonpertubative properties of (anti-) quarks and mesonic composites in a Quark-Gluon Plasma at temperatures $T \simeq 1.2$-$2\,T_c$. Our key ingredient to describe the q-$\bar{q}$ interaction in the QGP was a driving kernel (potential) extracted from unquenched finite-T lattice QCD calculations for the free energy of a heavy-quark pair, supplemented with corrections for relativistic motion. Our main objective was to go beyond earlier applications to bound states by solving the scattering problem thereby accounting for absorptive effects (finite imaginary parts). The self-consistent set of single-quark Dyson and two-body scattering equations has been solved by numerical iteration employing a nonrelativistic reduction of the Bethe-Salpeter equation in connection with a quasi-particle approximation for the quark propagators. One of our main new findings is that the lQCD potentials (dynamically) generate S-wave resonance states *above* the q-$\bar{q}$ threshold up to temperatures of $\sim 2\ T_c$. These resonances (assumed to occur with a degeneracy corresponding to "π"- and "ρ"-mesons), in turn, play a key role in inducing large quark scattering rates (=imaginary parts

of the quark self-energy) as indicated by single-particle widths of $\Gamma \simeq 200$ MeV at temperatures around 1.5 T_c. At the same time, significant (positive) real parts arise from repulsive interactions in the color-octet channel entailing thermal masses of up to ∼150 MeV. We expect that additional contributions to the quark mass of ∼250 MeV (induced, *e.g.*, by interactions with thermal gluons as parametrized in quasiparticle models) will be necessary to account for the QGP EoS computed in lattice QCD. Nevertheless, especially at low momenta, the quark widths are comparable to the thermal masses, which could be indicative for liquid-like properties of the QGP at moderate temperatures.

Our analysis suggests several directions for future work. First, the accuracy of our approximations should be scrutinized. This includes improving upon the quasiparticle approximation of the quark spectral function by implementing its off-shell (energy-) dependence (as, *e.g.*, carried out in Ref. [45] for a hot pion gas), most notably at low energies to incorporate bound-state contributions to the quark self-energy. The scattering equation ought to be extended to finite total 3-momentum of the mesonic composites. Even though we expect the q-$\bar{q}$ channel to constitute a major part of the in-medium interaction, a more complete treatment including q-q and q-g channels is desirable. It is also conceivable that processes of the type $q\bar{q} \to Mg$ (inverse gluon-dissociation; M: mesonic state) could be significant, as they render bound states accessible in (on-shell) 2-body scattering. In a broader context, the underlying EoS of the interacting system needs to be investigated, which is obviously not an easy task. On the phenomenological side, to address the problem of early equilibration at RHIC, it will be of great interest to calculate the thermal equilibration timescales for (anti-) quarks based on the resonant scattering amplitudes found here (*e.g.*, within a Fokker-Planck equation). The elastic scattering rates of around $1/(\mathrm{fm})/c$ as found in this work, together with the isotropic angular dependence inherent in S-wave rescattering, look promising. For gluons the situation could be more involved since, besides bound states as suggested in Ref. [21], other thermalization mechanisms might be operative, e.g., $gg \leftrightarrow ggg$ processes [46, 47]. In this respect, charm quarks are of particular importance, as their number is presumably frozen after primordial production, and genuine 2→3 processes are absent. Indeed, the recent analysis of Ref. [10] has shown that "D"-meson resonances in the QGP can accelerate thermal relaxation times obtained from pQCD by a factor of ∼3. A rather straightforward extension of our approach to the heavy-light sector should therefore be pursued. The formation of mesonic composites in the cooling QGP phase of a heavy-ion collision could furthermore serve as a "pre-hadronization" mechanism, and thus improve phenomenologically successful quark-coalescence models at RHIC [48, 49, 50] (*e.g.*, with respect to the question of energy conservation). Significant future efforts will be required to possibly develop such a scheme into a quantitative phenomenology. Further progress will also reside on increasing information from finite-T lattice QCD to provide both input and constraints to a many-body approach as presented here. Clearly, a thorough understanding of the intricate properties of the strongly interacting matter above T_c, and its implications for ultrarelativistic heavy-ion experiments, is an exciting future task.

Acknowledgement
We are grateful to P. Petreczky for sending us the data files of the unquenched lattice results for the free energies used in this work. One of us (RR) has been supported in part by a U.S. National Science Foundation CAREER award under grant PHY-0449489. The work of MM has been supported in part by U.S. Department of Energy (D.O.E.) under cooperative research agreement

#DE-FC02-94ER40818.

---

[1] R. Baier, A. H. Mueller, D. Schiff, and D. T. Son, Phys. Lett. **B502**, 51 (2001).
[2] P. F. Kolb and U. Heinz (2003), nucl-th/0305084.
[3] D. Teaney, J. Lauret, and E. V. Shuryak, Phys. Rev. Lett. **86**, 4783 (2001).
[4] T. Hirano, J. Phys. **G30**, S845 (2004).
[5] S. Datta, F. Karsch, P. Petreczky, and I. Wetzorke, Nucl. Phys. Proc. Suppl. **119**, 487 (2003).
[6] M. Asakawa and T. Hatsuda, Phys. Rev. Lett. **92**, 012001 (2004), hep-lat/0308034.
[7] T. Umeda, K. Nomura and H. Matsufuru, Eur. Phys. J. C **39S1**, 9 (2005).
[8] F. Karsch and E. Laermann (2003), hep-lat/0305025.
[9] M. Asakawa and T. Hatsuda, Nucl. Phys. **A721**, 869 (2003).
[10] H. van Hees and R. Rapp Phys. Rev. C **71**, 034907 (2005).
[11] T. Hatsuda and T. Kunihiro, Phys. Lett. **B145**, 7 (1984).
[12] T. Hatsuda and T. Kunihiro, Phys. Rev. Lett. **55**, 158 (1985).
[13] T. Schäfer and E. V. Shuryak, Phys. Lett. **B356**, 147 (1995).
[14] X. Li, H. Li, C. M. Shakin, and Q. Sun, Phys. Rev. C **69**, 065201 (2004).
[15] W. M. Alberico, A. Beraudo, and A. Molinari, Nucl. Phys. **A750**, 359 (2005).
[16] S. Digal, P. Petreczky, and H. Satz, Phys. Rev. D **64**, 094015 (2001).
[17] C.-Y. Wong (2004), hep-ph/0408020.
[18] A. Mocsy and P. Petreczky (2004), hep-ph/0411262.
[19] E. V. Shuryak and I. Zahed, Phys. Rev. C **70**, 021901 (2004).
[20] G. E. Brown, C.-H. Lee, M. Rho, and E. Shuryak, Nucl. Phys. **A740**, 171 (2004).
[21] E. V. Shuryak and I. Zahed, Phys. Rev. D **70**, 054507 (2004).
[22] P. Petreczky, F. Karsch, E. Laermann, S. Stickan, and I. Wetzorke, Nucl. Phys. Proc. Suppl. **106**, 513 (2002).
[23] O. Philipsen, Phys. Lett. **B535**, 138 (2002).
[24] O. Kaczmarek, F. Karsch, P. Petreczky, and F. Zantow, Phys. Lett. **B543**, 41 (2002).
[25] O. Kaczmarek, F. Karsch, F. Zantow, and P. Petreczky, Phys. Rev. D **70**, 074505 (2004).
[26] O. Kaczmarek, F. Karsch, P. Petreczky, and F. Zantow, Nucl. Phys. Proc. Suppl. **129**, 560 (2004).
[27] P. Petreczky, private communcation (2004).
[28] F. Karsch, M. T. Mehr, and H. Satz, Z. Phys. **C37**, 617 (1988).
[29] P. Petreczky and K. Petrov, Phys. Rev. D **70**, 054503 (2004).
[30] S. Digal, Proceedings of the Int. Conference on "Hard and Electromagnetic Probes of High-Energy Heavy-Ion Collisions" (Ericeira, Portugal, Nov. 4-10, 2004) (2004), hep-ph/0505193.
[31] O. Jahn and O. Philipsen, Phys. Rev. D **70**, 074504 (2004).
[32] G. E. Brown, Philos. Mag. **43**, 467 (1952).
[33] P. Levai and U. W. Heinz, Phys. Rev. C **57**, 1879 (1998).
[34] R.A. Schneider and W. Weise, Phys. Rev. C **64**, 055201 (2001).
[35] A. Peshier, B. Kampfer, and G. Soff, Phys. Rev. D **66**, 094003 (2002).
[36] J.-P. Blaizot, E. Iancu, and A. Rebhan (2003), hep-ph/0303185.
[37] U. Kraemmer and A. Rebhan, Rept. Prog. Phys. **67**, 351 (2004).
[38] R. Blankenbecler and R. Sugar, Phys. Rev. **142**, 1051 (1966).
[39] R. H. Thompson, Phys. Rev. D **1**, 110 (1970).
[40] M. Asakawa, T. Hatsuda, and Y. Nakahara, Nucl. Phys. **A715**, 863 (2003).
[41] M. I. Haftel and F. Tabakin, Nucl. Phys. **A158**, 1 (1970).
[42] L. Grandchamp, R. Rapp and G.E. Brown, Phys. Rev. Lett. **92**, 212301 (2004).
[43] A. Peshier and W. Cassing (2005), hep-ph/0502138.
[44] M. H. Thoma, J. Phys. **G31**, L7 (2005).
[45] R. Rapp and J. Wambach, Phys. Lett. **B351**, 50 (1995).
[46] S. M. H. Wong, Nucl. Phys. **A607**, 442 (1996); Phys. Rev. C **54**, 2588 (1996).
[47] Z. Xu and C. Greiner (2004), hep-ph/0406278.
[48] R. J. Fries, S. A. Bass, and B. Muller, Phys. Rev. Lett. **94**, 122301 (2005).

[49] V. Greco, C. M. Ko, and P. Levai, Phys. Rev. Lett. **90**, 202302 (2003).
[50] R. C. Hwa and C. B. Yang, Phys. Rev. C **67**, 034902 (2003).